www.nephropathol.com DOI: 10.34172/jnp.2021.17 J Nephropathol. 2021;10(2):e17

Journal of Nephropathology

Mesangial matrix expansion in a novel mouse model of diabetic kidney disease associated with the metabolic syndrome

Elisabet Van Loon[1,2], Joseph Pierre Aboumsallem[3], Evelyne Lerut[4], Marija Bogojevic[5], Aleksandar Denic[5], Walter Park[6], Ilayaraja Muthuramu[3], Mudit Mishra[3], Mark Stegall[6], Maarten Naesens[1,2*], Bart De Geest[3]

[1]Nephrology and Renal Transplantation Research Group, Department of Microbiology, Immunology and Transplantation, KU Leuven, Leuven, Belgium
[2]University Hospitals Leuven, Department of Nephrology and Renal Transplantation, Leuven, Belgium
[3]Centre for Molecular and Vascular Biology, Department of Cardiovascular Sciences, KU Leuven, Leuven, Belgium
[4]Department of Imaging and Pathology, Division of Translational Cell and Tissue Research, KU Leuven, Leuven, Belgium
[5]Division of Nephrology and Hypertension, Mayo Clinic, Rochester, Minnesota, USA
[6]William J von Liebig Center for Transplantation and Clinical Regeneration, Mayo Clinic, Rochester, Minnesota, USA

ARTICLE INFO

Article type:
Original Article

Article history:
Received: 8 August 2020
Accepted: 5 September 2020
Published online: 17 September 2020

Keywords:
Diabetic kidney disease
Metabolic syndrome
Mesangial matrix expansion

ABSTRACT

Introduction: The evolution of structural changes of diabetic nephropathy in human kidneys is not well documented. Instead, rodent models are used to study diabetic nephropathy in greater detail. However, all rodent models to date are subject to important limitations, and not representative for the more complex human setting where type 2 diabetes mellitus is often accompanied by the metabolic syndrome, induced by a high-fructose western diet.

Objectives: To evaluate whether a novel mouse model of metabolic syndrome could be used as valid model for preclinical studies on diabetic nephropathy.

Materials and Methods: We established a model of type 2 diabetes mellitus induced by a high-sucrose/high-fat (HSHF) diet in female LDL-receptor knockout C57BL/6J mice and used manual morphometry to examine the renal histological changes in this model.

Results: The HSHF diet induced a metabolic syndrome with weight gain, hyperinsulinemia, insulin resistance, type 2 diabetes mellitus, and hyperlipidemia. After 16 weeks on the HSHF diet, morphometric examination of kidney biopsies demonstrated increased mesangial matrix expansion, no glomerulosclerosis, and only discrete morphological changes in glomeruli. Mesangial matrix expansion was highly correlated with biological features of the metabolic syndrome.

Conclusion: We describe a novel, accessible mouse model with features of the metabolic syndrome and development of mesangial matrix expansion. This model is comparable to the human setting and could serve as a relevant experimental model for nephropathy associated with type 2 diabetes mellitus. By assessing both morphological and morphometric features we demonstrated the increased sensitivity and more detailed evaluation of manual morphometry over visual estimation by light microscopy.

Implication for health policy/practice/research/medical education:
In a novel mouse model representative of the metabolic syndrome induced by a high-sucrose high-fat diet, morphometric examination of kidney biopsies demonstrated increased mesangial matrix expansion, while only discrete morphological changes in glomeruli were noticed. This novel, accessible mouse model, comparable to the human setting could serve as a relevant experimental model for nephropathy associated with type 2 diabetes mellitus. By assessing both morphological and morphometric features we demonstrated the increased sensitivity of manual morphometry over visual estimation by light microscopy.

Please cite this paper as: Van Loon E, Aboumsallem JP, Lerut E, Bogojevic M, Denic A, Park W. Mesangial matrix expansion in a novel mouse model of diabetic kidney disease associated with the metabolic syndrome. J Nephropathol. 2021;10(2):e21. DOI: 10.34172/jnp.2021.17.

*Corresponding author: Maarten Naesens, MD, PhD, Email: maarten.naesens@kuleuven.be

Original Article

Introduction

Diabetic nephropathy is a major cause of chronic kidney disease (1). The evolution of diabetic nephropathy is hallmarked by functional changes (proteinuria, hyperfiltration) and structural changes (glomerular basement membrane thickening, mesangial matrix expansion, glomerulosclerosis) (2-4). In humans with diabetes, kidneys are typically enlarged, and associated with worse renal outcome (5). The mechanism behind this enlargement is not well understood and could be related to compensatory hypertrophy, or excessive accumulation of abnormal substrates, or renotrophic factors(6). The clinical diagnosis of diabetic nephropathy in humans does not require histological confirmation. Since only few histological studies were performed in native kidneys of patients with a variable duration of (mainly type 1) diabetes (7,8), the dynamics of the structural changes of diabetic nephropathy in native kidneys are not well documented.

In a previous study in renal allografts, with the unique opportunity to study the histological evolution of diabetic nephropathy in sequential protocol biopsies, mesangial matrix expansion occurred more frequently in patients with pre-transplant (primarily type 2) diabetes mellitus, but independently of glycated haemoglobin levels (9). We hypothesized that the rapid onset of mesangial matrix expansion could be due to effects of diabetes on advanced glycation end product formation, inflammation, hemodynamics, and oxidative stress (10-12). Also, dyslipidemia, hemodynamic factors, insulin resistance and other metabolic features of the metabolic syndrome could play a role in the development of mesangial matrix expansion (13). Our previous study and other studies also showed mesangial matrix expansion to be related to ageing (9,14-16). In the human setting, where many of these factors co-occur, especially in patients with type 2 diabetes and the metabolic syndrome, it remains unclear which factors are most contributing to the mesangial matrix changes.

Since there is a considerable difference in the metabolism of glucose and fructose (17), it was hypothesized that fructose may have a unique contribution to the etiology of obesity, type 2 diabetes mellitus, and cardiovascular disease (18,19). High-fructose-containing diets have also been linked to renal injury and exaggeration of diabetic nephropathy in both humans and animals (20-25). To study this in more controlled settings, we recently established a model of type 2 diabetes mellitus induced by a high-sucrose/high-fat (HSHF) diet in female LDL-receptor knockout C57BL/6 J mice (26). These mice were given a HSHF diet to induce the metabolic syndrome and type 2 diabetes mellitus, or a standard chow diet (SC). The HSHF diet induced a metabolic syndrome with gain of weight, hyperinsulinemia, insulin resistance, type 2 diabetes mellitus, and hyperlipidemia (26). Also, diabetic cardiomyopathy with increased heart weight and more specifically features of heart failure with preserved ejection fraction developed upon the HSHF diet (26). Additionally, a gain in kidney weight was observed, consistent with the enlargement in humans with diabetic nephropathy (26). This finding led us to hypothesize that this mouse model also had histopathological features of diabetic nephropathy.

Recently, Denic et al (27) demonstrated that manual morphometry performed on surveillance biopsies five years post-transplantation better predicted subsequent renal allograft failure than the visual scoring by a pathologist. More importantly, in a subset of patients without chronic glomerulopathy, morphometric measure of mesangial matrix expansion (but not the semiquantitative histological mm score) was identified as predictor of allograft failure. This suggests that visual estimation likely underestimates the evolution of mesangial expansion associated with diabetes mellitus.

Objectives

In this study, we aimed to evaluate whether our recently described model of diabetes mellitus type 2 induced by an HSHF diet in female LDL-receptor knockout C57BL/6 mice could be used as valid model for preclinical studies on diabetic nephropathy, using manual morphometry to examine the renal histological changes in this model.

Materials and Methods

Animal model

At the semi-specific pathogen free facility of KU Leuven, C57BL/6J low-density lipoprotein receptor deficient ($LDLr^{-/-}$) mice (purchased from Jackson Laboratories (Bar Harbor, ME, USA)) were bred. All mice were female. All mice were fed a standard chow (SC) diet (Sniff Spezialdiäten GMBH, Soest, Germany) or an HSHF western diet (Test Diet 58Y1, TestDiet®, London, United Kingdom). Metabolizable energy from the SC diet is 13.5 MJ/kg (9 kJ% fat, 24 kJ% protein, 67 kJ% carbohydrates), and from the HSHF diet is 19.5 MJ/kg (46.4 kJ% fat, 17.6 kJ% protein, 36.0 kJ% carbohydrates). In the HSHF diet, mono- and disaccharides consisted of high-fructose corn syrup-55 (17.5%) and sucrose (17.5%) (28). The SC diet was continued in N=10/30 of the mice whereas in the other 20/30 mice the HSHF diet was initiated at the age of 12 weeks and continued for 16 weeks. At the age of 28 weeks (=end of study), all mice were alive and included for analysis (26).

Biochemistry

To obtain blood the retro-orbital plexus was punctured

and anticoagulated with trisodium citrate. Plasma was then isolated by centrifugation at 1100× *g* for 10 minutes and stored at –20°C. Methods for quantification of plasma levels of free fatty acids, insulin and tumor-necrosis factor alfa (TNF-α) were previously described (26). In a subset of mice (n=10 of the 20 HSHF diet LDLr$^{-/-}$ mice) data on insulin levels, TNF-α and adiponectin were measured, and fatty acids levels were measured in n=18 of the 20 HSHF diet LDLr$^{-/-}$ mice, using the techniques previously described. The homeostasis model assessment-insulin resistance (HOMA-IR) index was calculated as measure for insulin resistance using the formula: HOMA-IR=Insulin$_0$ (μU/mL) x Glucose$_0$ (mmol/L)/22.5(29).

Morphology/Morphometry

Paraffin-embedded left and right kidney sections were stained with periodic acid-Schiff and Jones methenamine silver stain. All light microscopic images were evaluated by one pathologist (EL), and the histological changes were described in the glomerular, tubulo-interstitial and vascular renal compartments. In addition, morphometric measurements were performed at Mayo Clinic, Rochester, USA. First, all biopsy slides were scanned into high-resolution digital images (Aperio® AT2 system scanner, Leica Microsystems, Inc., Buffalo Grove, IL; http://www.aperio.com). Biopsy images were morphometrically analyzed by investigators masked to study group to minimize bias. The scanned digital images were magnified with ImageScope software (version 12.2.2.5015 Aperio®) onto a large pen sensitive screen. Only one kidney per mouse was selected for morphometric analysis. Mesangial expansion was assessed in glomeruli in a sampled cortex (approximately 20-25% of the total cortex) (Figure 1A). At higher magnification, every glomerular cross-sectional profile in the sampled cortex was traced to obtain the number and area of glomeruli (Figure 1B). Then, in each traced glomerulus, areas of mesangial expansion were also traced (Figure 1C). Mesangial hypercellularity was defined as ≥3 cells in the mesangium. The percent of mesangial matrix expansion was calculated as the sum of all mesangial matrix expansion areas over the area of all traced glomeruli (including non-affected), as previously reported (27). Furthermore, as additional measure we calculated percent of glomeruli affected with mesangial expansion. The mean cross-sectional tubular area was obtained in a 1 mm^2 of sampled cortex, approximately equidistant between the capsule and cortico-medullary junction (Supplementary file 1, Figure S1A), using the same approach previously applied to kidney donor biopsies (30). For glomerular morphometry measures, we traced the whole cortex and all glomeruli on a single kidney (Supplementary file 1, Figure S1B). From these measurements we calculated mean glomerular area and mean glomerular area density, and using stereology models (31) we calculated mean glomerular volume and glomerular volumetric density.

Ethical issues

All experimental procedures in animals were executed in accordance with protocols approved by the Institutional Animal Care and Research Advisory Committee of KU Leuven (Approval number P191/2015).

Statistical analysis

The investigators who performed the analyses were blinded to group allocation. Variables are displayed as mean ± standard deviation. Morphometric differences between the two groups were tested with Kruskal-Wallis tests. Pearson correlation analysis was used to assess associations between continuous variables and histological lesions. For correlation analysis, samples with missing values were excluded. A correlation matrix was constructed using Pearson correlation coefficients. The SAS 9.4 software (SAS Institute) and R (version 3.6.3, R core team, 2014) were used for statistical analysis. For data presentation

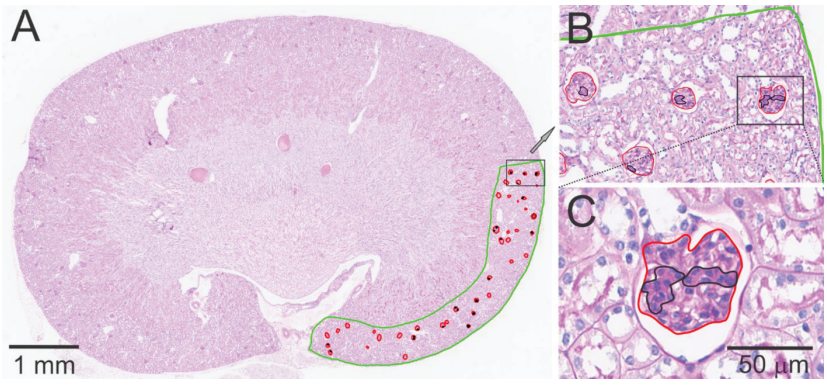

Figure 1. Morphometric analysis. Mesangial expansion was assessed in glomeruli in a sampled cortex (approximately 20-25% of the total cortex) (**A**). At higher magnification, every glomerular cross-sectional profile in the sampled cortex was traced to obtain the number and area of glomeruli (**B**). Then, in each traced glomerulus, areas of mesangial expansion were also traced (**C**).

GraphPad Prism (version 8; GraphPad Software, San Diego, CA) was used.

Results

Study population characteristics

Biological characteristics of the C57BL/6J LDLr$^{-/-}$ mice at 28 weeks (end of study) were described previously(26). At the end of the study (28 weeks), mice on the HSHF diet (n=20) developed features of the metabolic syndrome with gain of weight, hyperglycemia, hyperinsulinemia with increased HOMA-IR index and hyperlipidemia compared to mice fed the SC diet (n=10). Increased levels of TNF-α levels were observed in mice fed the HSHF diet compared to the SC diet. No significant differences were found in free fatty acid or adiponectin levels (Figure 2A, Table 1).

Morphological findings

Kidney weights were different between the two groups (Table 1). Morphological evaluation of kidneys from C57BL/6J LDLr$^{-/-}$ mice fed the HSHF (n=20) or SC (n=10) diet showed discrete changes. The intraglomerular nuclei (mesangium, visceral epithelium and endothelium) of mice are somewhat larger compared to humans, which gave the impression of crowded glomeruli. On a higher magnification, using criteria for assessment of human glomeruli, discrete mesangial matrix expansion and hypercellularity was seen in some slides of mouse kidneys. These changes were more often found in the mice fed the HSHF diet (n=11/20; 55%) compared to 30% (n=3/10) in mice fed the SC diet. By light microscopy, no glomerulosclerosis, thickening of the glomerular basement membrane, interstitial or vascular lesions were observed.

Morphometry findings

Morphometric analysis confirmed these mesangial matrix changes in the HSHF fed mice more robustly. There were no differences in size or density of the glomeruli. There was no difference in glomerulosclerosis between the two groups; neither in tubular size measurement (Table 1). The percentage of mesangial matrix expansion was significantly greater in mice fed the HSHF diet compared to the SC

Table 1. Biological and morphometric measurements in the two experimental groups

Characteristic	HSHF diet (n = 20)	SC diet (n = 10)	P value
Biological measurements			
Body weight, g	33.89 ± 4.04	22.77 ± 1.99	<0.0001
Kidney weight, mg	297.9 ± 48.6	252.3 ± 19.4	0.001
Plasma glucose, mmol/L	8.28 ± 1.12	6.40 ± 0.30	<0.0001
Plasma insulin, pmol/L	276.7 ± 52.44*	56.25 ± 11.04	<0.0001
HOMA-IR index	17.07 ± 3.40*	2.66 ± 0.49	<0.0001
TNF-α, pg/mL	319.0 ± 146.6*	42.3 ± 10.6	0.0002
Free fatty acids, mmol/L	0.58 ± 0.12*	0.51 ± 0.12	0.13
Adiponectin, ng/mL	5574.4 ± 1860.1 *	5969.9 ± 932.1	0.56
Cholesterol, mg/dL*	464.3 ± 79.3	212.5 ± 32.9	<0.0001
Morphometric measurements			
Kidney weight at 28 weeks, sum of left and right kidney, mg	297.9 ± 48.6	252.3 ± 19.4	0.008
Morphometric measures on sampled cortex			
Sampled cortex area, mm^2	3.1 ± 0.7	3.0 ± 0.7	0.69
Number of glomeruli	46 ± 12	40 ± 7	0.15
% of mesangial matrix expansion	3.2 ± 1.7	1.2 ± 0.8	0.004
% of glomeruli with ME	25.5 ± 11.0	13.5 ± 7.5	0.005
Mean cross-sectional tubular area, per 1000 μm^2	1.87 ± 0.36	2.03 ± 0.24	0.15
Morphometric measures on whole cortex			
Cortex area, mm^2	16.3 ± 4.1	16.6 ± 4.5	0.86
Number of glomeruli	217 ± 37	229 ± 60	0.83
Mean glomerular area, per 1000 μm^2	2.41 ± 0.32	2.46 ± 0.23	0.76
Mean glomerular volume, mm^3	0.00016 ± 0.00003	0.00017 ± 0.00002	0.75
Glomerular area density, per mm^2	13.8 ± 3.0	14.0 ± 1.4	0.60
Glomerular volumetric density, per mm^3	206.5 ± 53.9	204.4 ± 26.2	0.66

TNF, tumor necrosis factor; HOMA-IR, homeostasis model assessment-insulin resistance; ME, mesangial expansion
*Missing data (N=10 missing for plasma insulin, HOMA-IR index, TNF-α, adiponectin and N=2 missing for free fatty acids. N=12 missing for cholesterol).

diet, as well as the percentage of non-sclerosed glomeruli with mesangial matrix expansion (Table 1, Figure 2B).

Correlation with biological data

A Pearson correlation matrix showed that mesangial matrix expansion measures were correlated with biological markers of the metabolic syndrome (Figure 3). The percentage of mesangial matrix expansion correlated with body weight ($\rho = 0.74$, $P = 0.0005$), insulin levels ($\rho = 0.51$, $P = 0.03$) and HOMA-IR ($\rho = 0.52$, $P = 0.03$), but not with plasma glucose without consideration of insulin levels ($\rho = 0.46$, $P = 0.06$). Mesangial matrix expansion positively correlated with TNF-α levels ($\rho = 0.69$, $P = 0.002$) and total cholesterol levels ($\rho = 0.57$, $P = 0.01$). No significant correlations were found with free fatty acids or adiponectin levels ($\rho = 0.11$, $P = 0.65$ and $\rho = -0.009$, $P = 0.97$). Results were similar for the percentage of non-sclerosed glomeruli with mesangial matrix expansion. None of the other histological measurements (mean cross-sectional tubular area, mean glomerular area, mean glomerular volume, glomerular area density or glomerular volumetric density) correlated significantly with these metabolic parameters. Linear regression analysis demonstrated a statistically significant association between percentage of mesangial matrix expansion and body weight (slope = 0.16, $P = 0.0007$), TNF-α (slope = 0.007, $P = 0.0006$), insulin (slope = 0.007, $P = 0.02$), the HOMA-IR index (slope = 0.12, $P = 0.01$) and total cholesterol (slope = 0.007, $P = 0.01$) (Figure 2C).

Discussion

In this study, we present a novel mouse model of the metabolic syndrome with mesangial matrix expansion compatible with diabetic nephropathy. This model better reflects the human disease with an accumulation of metabolic risk factors in type 2 diabetic patients than e.g. the streptozocin-induced mouse model of pancreatic beta cell toxicity. Patients often fulfil criteria of the metabolic syndrome with increased abdominal obesity together with elevated fasting glucose levels, insulin resistance, elevated blood pressure, and plasma lipids, as was also the case in our mouse model. We demonstrated that the glomerular changes in this mouse model associated with insulin resistance and TNF-α levels, but not with plasma glucose levels, free fatty acid levels or adiponectin.

Mesangial matrix expansion has been associated with

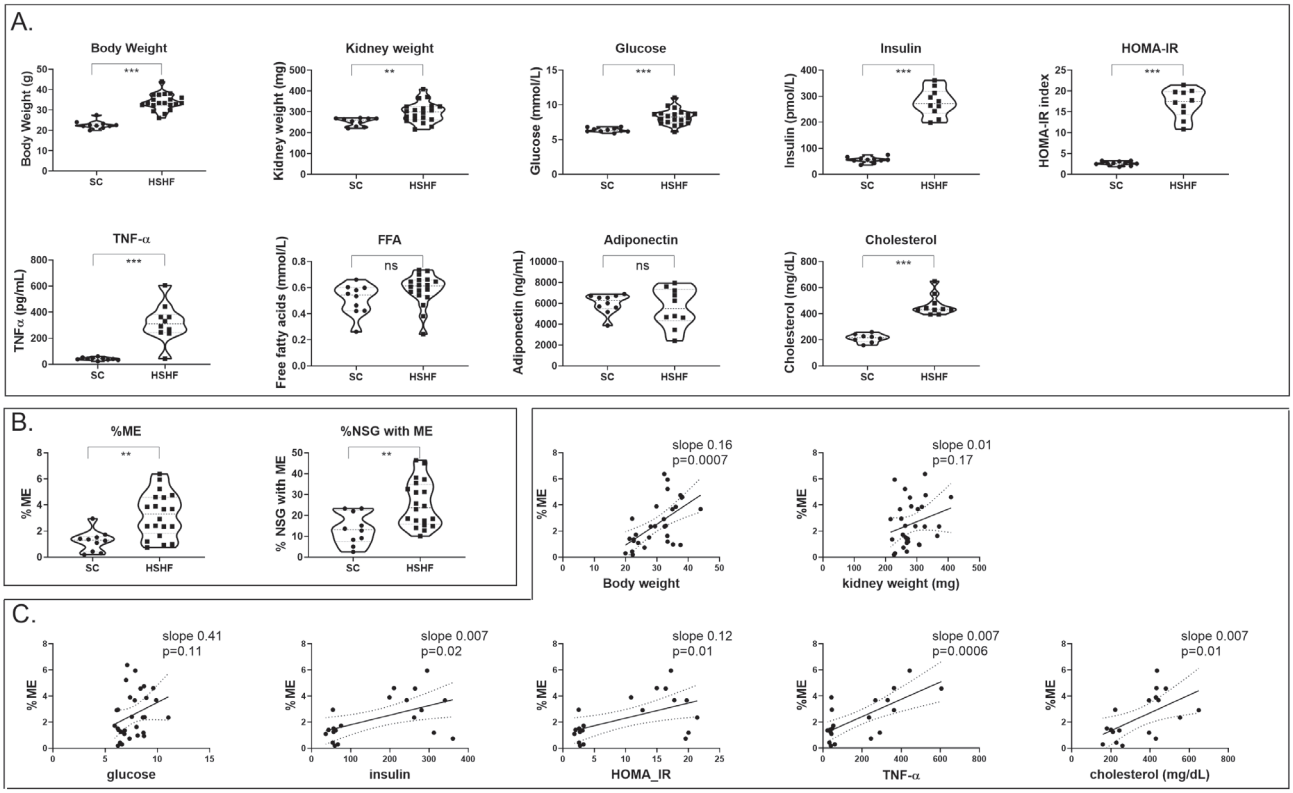

Figure 2. (A) Violin plots comparing biological variables across the standard chow (SC) and high sucrose high fat (HSHF) diet. **(B)** Violin plots comparing morphometric measurements across the SC and HSHF diet. **(C)** Linear regression between percentage of mesangial matrix expansion and biological parameters. HOMA-IR: homeostasis model assessment-insulin resistance index; TNF-α: tumor-necrosis factor α; FFA: free fatty acids; %ME: percentage of mesangial matrix expansion; %NSG with ME: percentage of non-sclerosed glomeruli with mesangial matrix expansion. $^{*}P < 0.05$, $^{**}P < 0.01$, $^{***}P < 0.001$, ns = not significant

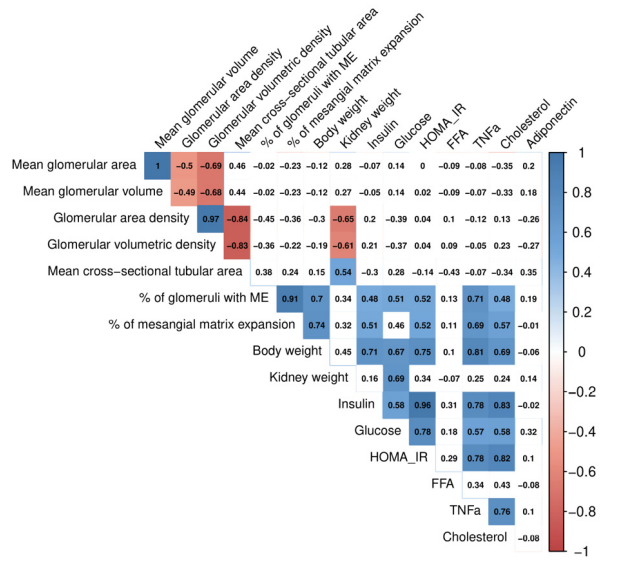

Figure 3. Correlation matrix of morphometric and biological observations. Pearson correlation coefficients are given. Blank boxes indicate non-significant correlations ($P>0.05$). All cases with missing data were omitted from the analysis. HOMA-IR: homeostasis model assessment-insulin resistance index; TNF-α: tumor-necrosis factor α; FFA: free fatty acids; ME: mesangial matrix expansion.

(accelerated) renal ageing (9,14-16) Nevertheless, late changes in diabetic nephropathy, such as glomerulosclerosis or arteriolar hyalinosis, were not observed in this study, in contrast to the mesangial matrix effects. This makes this model ideally suited to study the glomerular changes caused by type 2 diabetes, rather than the general ageing changes. Many rodent models for type 2 diabetes and obesity have been described (32), ranging from monogenic models defective in leptin signalling ($Lep^{ob/ob}$ mice, $Lepr^{db/db}$ mice and ZDF rats) to polygenic mouse models of diet-induced obesity, glucose intolerance and diabetes (C57BL/6J mouse strain (33), C57BL/6N , New Zealand Obese (NZO), TALLYHO/Jng and KK mice and also non genetic chemical-induced animal models of diabetes (like the high-fat diet/streptozotocin-treated (HFD/STZ) animal model). For an overview of mouse models of diabetic nephropathy we refer to the detailed reviews by Alpers et al and Breyer et al (34,35). In contrast to our model, most mouse models for type 2 diabetes and diabetic nephropathy report glomerulosclerotic changes. Mouse models of diabetes mimicking early morphological changes of human diabetic nephropathy, mostly mesangial matrix expansion and sometimes, podocyte loss, include *db/db* and Akita mice (35). However, these models have limitations. *db/db* mice with leptin deficiency are infertile, making the breeding of mice in sufficient numbers for interventional studies expensive and labor intensive. Akita mice on the other hand are more suitable as a model for type 1 diabetes and demonstrate IgA deposition (36), which is a confounding the interpretation of the observed mesangial matrix expansion. There are only few models that mimic morphological features of both early and late diabetic nephropathy; the most robust seem to be those with deficiency of eNOS, OVE26 FVB mice, and BTBR *ob/ob* (35). All mouse models available to date are subject to important limitations and better models of diabetic nephropathy are still needed for deepening our mechanistic insight or for testing novel therapeutic interventions.

The mouse models of diabetes that mimic early morphological changes of human diabetic nephropathy, mainly mesangial matrix expansion, include db/db and Akita mice (35). Interestingly, C57BL/6 mice have been found to be less susceptible to diabetic nephropathy changes (34, 35). Balmer et al found that B6 mice display less renal hypertrophy (kidney weight: body weight) response to diabetes compared to mice from another strain (FVB). When they introgressed B6 regions to the FVB strain, these regions protected against diabetes-induced increased kidney weight and glomerulosclerosis (37).

C57BL/6 is a common inbred strain of mice, widely used due to the availability of congenic strains, easy breeding, and robustness.

In our novel mouse model, we found strong correlations between the mesangial matrix measurements and TNF-α levels, a pro-inflammatory cytokine. The association between mesangial matrix expansion and oxidative stress/inflammation was illustrated before (13,38). Also, studies in mice using glucose-sodium transporter blockade with sodium-glucose cotransporter-2 (SGLT2) inhibitors demonstrated prevention and reversal of mesangial matrix expansion by dampening hyperglycemia-induced oxidative stress and inflammation (39,40). This effect was even demonstrated to be independent of its glucose-lowering effect (41,42). In a previous study in kidney transplant recipients, we found apparent independence of glycemic control in developing mesangial matrix expansion (9). Reflecting these findings in humans, also in our novel mouse model, mesangial matrix expansion was not significantly correlated with glucose levels but rather with the metabolic measures of insulin resistance and inflammation. Insulin might indeed be a more important determinant of mesangial matrix expansion than plasma glucose levels alone, as suggested by the higher mesangial matrix expansion incidence in insulin-dependent diabetic patients (9), and by the finding that insulin prevents diabetes-induced hyperfiltration and proteinuria, but could not prevent glomerular growth, and even induced mesangial expansion (43). This might reflect an effect of insulin treatment itself, with more hypoglycemic hyperinsulinemic episodes, a trophic effect of insulin, and

more fluctuating glucose profiles.

By assessing both morphological and morphometric features, we demonstrated the increased sensitivity and more detailed evaluation of manual morphometry over visual estimation by light microscopy. These findings are in agreement with the recent study of 175 kidney transplant patients in which semiquantitative lesion scores were compared to morphometric surrogates on 5 year surveillance biopsies (27). Although semiquantitative lesion scores and morphometry overall had significant correlation with each other, at best this correlation was modest. However, most importantly, morphometry performed better in predicting subsequent graft loss better than semiquantitative pathological scoring in terms of model discrimination (c-statistic). Moreover, when analysis was performed in a subset of patients whose biopsies did not feature chronic glomerulopathy, manual morphometry not only had a better c-statistic, but also identified additional lesions that were predictive of graft loss (e.g. mesangial expansion and luminal stenosis) (27). Finally, this study also showed how compared to visual estimation, manual morphometry was more reproducible. This is in agreement with recent studies that showed better reproducibility and reliability when scanned slides were analyzed compared to traditional glass slides on light microscopy (44,45).

There are some limitations to this study. Notably, the morphological findings cannot fully explain the gain in weight in these mouse kidneys. Steatosis might possibly be playing a role in this weight gain, however this could not be examined due to the fixation technique (paraffin embedded slides). Furthermore, there are considerable confounders in this study, especially the collinearity of the glucose metabolism parameters with very high cholesterol levels in this LDL-receptor knockout mouse model. Iacobini et al described mesangial matrix expansion in response to lipid toxicity (13), and our data show correlation of mesangial matrix expansion with total cholesterol, however we found no significant correlations between free fatty acid or adiponectin levels and mesangial matrix expansion measures. Also, Bornfeldt et al described no effect of hyperlipidemia, induced by LDL-R degradation, on mesangial expansion or podocyte numbers in a BTBR mouse strain with leptin deficiency, which has emerged as one of the best models of advanced human diabetic kidney disease (46). Next, there are no standardized definitions of the metabolic syndrome or the HOMA-IR calculation in mice. There were also some missing values for some biological parameters in the HSHF diet group due to the initial study design. Moreover, no data on microalbuminuria was available since no urine samples were collected. Finally, plasma creatinine levels were not measured; therefore, no statements could be made on renal function/hyperfiltration.

In conclusion, we describe a novel, accessible mouse model with features of the metabolic syndrome and development of mesangial matrix expansion. This model is comparable to the human setting and could therefore serve as a relevant experimental model for nephropathy associated with type 2 diabetes mellitus.

Authors' contribution

JPA, IM, MM, and BDG conducted the mouse experiment and collected the clinical data. EL performed the light microscopic evaluation of the kidney biopsies. MB, AD, WP and MS performed the morphometric measurements on the kidney biopsy samples. EVL conducted the statistical analysis. EVL, JPA, MS, MN and BDG designed the study. EVL and MN drafted the manuscript and prepared figures. EVL, JPA, EL, MB, AD, WP, IM, MM, MS, MN and BDG contributed to the report and have read and agreed with the manuscript as written.

Conflicts of interest

The authors declare that they have no competing interests.

Ethical considerations

Ethical issues (including plagiarism, data fabrication, double publication) have been completely observed by the authors.

Data sharing statement

All of the data that underlie the results reported in this article (text, tables, figures, and appendices) can be made available on a collaborative basis following institutional review board approval, immediately following publication, without end date and for any purpose. Proposals should be directed at the corresponding author.

Funding/Support

EVL holds a fellowship grant (1143919N) from the Research Foundation Flanders (FWO). MN is a senior clinical investigator of the FWO (1844019N).

Supplementary Materials

Supplementary file 1 contains Figure S1A-B.

References

1. Webster AC, Nagler EV, Morton RL, Masson P. Chronic Kidney Disease. Lancet. 2017;389(10075):1238-52. doi: 10.1016/S0140-6736(16)32064-5.
2. Mauer SM, Steffes MW, Ellis EN, Sutherland DE, Brown DM, Goetz FC. Structural-functional relationships in diabetic nephropathy. J Clin Invest. 1984;74(4):1143-55. doi: 10.1172/JCI111523.

3. Adler S. Diabetic nephropathy: Linking histology, cell biology, and genetics. Kidney Int. 2004;66(5):2095-106. doi: 10.1111/j.1523-1755.2004.00988.x.
4. Tonneijck L, Muskiet MH, Smits MM, van Bommel EJ, Heerspink HJ, van Raalte DH, et al. Glomerular hyperfiltration in diabetes: mechanisms, clinical significance, and treatment. J Am Soc Nephrol. 2017;28(4):1023-39. doi: 10.1681/ASN.2016060666.
5. Rigalleau V, Garcia M, Lasseur C, Laurent F, Montaudon M, Raffaitin C, et al. Large kidneys predict poor renal outcome in subjects with diabetes and chronic kidney disease. BMC Nephrol. 2010;11:3. doi: 10.1186/1471-2369-11-3.
6. Kahn CB, Raman PG, Zic Z. Kidney size in diabetes mellitus. Diabetes. 1974;23(9):788-92. doi: 10.2337/diab.23.9.788.
7. Steinke JM, Sinaiko AR, Kramer MS, Suissa S, Chavers BM, Mauer M, et al. The early natural history of nephropathy in Type 1 Diabetes: III. Predictors of 5-year urinary albumin excretion rate patterns in initially normoalbuminuric patients. Diabetes. 2005;54(7):2164-71. doi: 10.2337/diabetes.54.7.2164
8. Mauer M, Zinman B, Gardiner R, Suissa S, Sinaiko A, Strand T, et al. Renal and retinal effects of enalapril and losartan in type 1 diabetes. N Engl J Med. 2009;361(1):40-51. doi: 10.1056/NEJMoa0808400.
9. Coemans M, Van Loon E, Lerut E, Gillard P, Sprangers B, Senev A, et al. Occurrence of diabetic nephropathy after renal transplantation despite intensive glycemic control: an observational cohort study. Diabetes Care. 2019;42(4):625-34. doi: 10.2337/dc18-1936.
10. Brownlee M. The pathobiology of diabetic complications: a unifying mechanism. Diabetes. 2005;54(6):1615-25. doi: 10.2337/diabetes.54.6.1615.
11. Dronavalli S, Duka I, Bakris GL. The pathogenesis of diabetic nephropathy. Nat Clin Pract Endocrinol Metab. 2008;4(8):444-52. doi: 10.1038/ncpendmet0894.
12. Valencia WM, Florez H. How to prevent the microvascular complications of type 2 diabetes beyond glucose control. BMJ. 2017;356:i6505. doi: 10.1136/bmj.i6505.
13. Iacobini C, Menini S, Ricci C, Scipioni A, Sansoni V, Mazzitelli G, et al. Advanced lipoxidation end-products mediate lipid-induced glomerular injury: role of receptor-mediated mechanisms. J Pathol. 2009;218(3):360-9. doi: 10.1002/path.2536.
14. Hill GS, Heudes D, Bariéty J. Morphometric study of arterioles and glomeruli in the aging kidney suggests focal loss of autoregulation. Kidney Int. 2003;63(3):1027-36. doi: 10.1046/j.1523-1755.2003.00831.x.
15. Verzola D, Gandolfo MT, Gaetani G, Ferraris A, Mangerini R, Ferrario F, et al. Accelerated senescence in the kidneys of patients with type 2 diabetic nephropathy. Am J Physiol Renal Physiol. 2008;295(5):F1563-73. doi: 10.1152/ajprenal.90302.2008.
16. Zhou XJ, Rakheja D, Yu X, Saxena R, Vaziri ND, Silva FG. The aging kidney. Kidney Int. 2008;74(6):710-20. doi: 10.1038/ki.2008.319.
17. Sun SZ, Empie MW. Fructose metabolism in humans - what isotopic tracer studies tell us. Nutr Metab (Lond). 2012;9(1):89. doi: 10.1186/1743-7075-9-89.
18. Malik VS, Hu FB. Fructose and cardiometabolic health: what the evidence from sugar-sweetened beverages tells us. J Am Coll Cardiol. 2015;66(14):1615-24. doi: 10.1016/j.jacc.2015.08.025.
19. Hannou SA, Haslam DE, McKeown NM, Herman MA. Fructose metabolism and metabolic disease. J Clin Invest. 2018;128(2):545-55. doi: 10.1172/JCI96702.
20. Bell RC, Carlson JC, Storr KC, Herbert K, Sivak J. High-fructose feeding of streptozotocin-diabetic rats is associated with increased cataract formation and increased oxidative stress in the kidney. Br J Nutr. 2000;84(4):575-82.
21. Sánchez-Lozada LG, Tapia E, Jiménez A, Bautista P, Cristóbal M, Nepomuceno T, et al. Fructose-induced metabolic syndrome is associated with glomerular hypertension and renal microvascular damage in rats. Am J Physiol Renal Physiol. 2007;292(1):F423-9. doi: 10.1152/ajprenal.00124.2006.
22. hoham DA, Durazo-Arvizu R, Kramer H, Luke A, Vupputuri S, Kshirsagar A, et al. Sugary soda consumption and albuminuria: results from the National Health and Nutrition Examination Survey, 1999-2004. PLoS One. 2008;3(10):e3431. doi: 10.1371/journal.pone.0003431.
23. Nakayama T, Kosugi T, Gersch M, Connor T, Sanchez-Lozada LG, Lanaspa MA, et al. Dietary fructose causes tubulointerstitial injury in the normal rat kidney. Am J Physiol Renal Physiol. 2010;298(3):F712-20. doi: 10.1152/ajprenal.00433.2009.
24. Toyoda K, Suzuki Y, Muta K, Masuyama T, Kakimoto K, Kobayashi A, et al. High fructose diet feeding accelerates diabetic nephropathy in Spontaneously Diabetic Torii (SDT) rats. J Toxicol Sci. 2018;43(1):45-58. doi: 10.2131/jts.43.45.
25. Nakagawa T, Johnson RJ, Andres-Hernando A, Roncal-Jimenez C, Sanchez-Lozada LG, Tolan DR, et al. Fructose Production and Metabolism in the Kidney. J Am Soc Nephrol. 2020;31(5):898-906. doi: 10.1681/ASN.2019101015.
26. Aboumsallem JP, Muthuramu I, Mishra M, De Geest B. Cholesterol-Lowering Gene Therapy Prevents Heart Failure with Preserved Ejection Fraction in Obese Type 2 Diabetic Mice. Int J Mol Sci. 2019;20(9). doi: 10.3390/ijms20092222.
27. Denic A, Morales MC, Park WD, Smith BH, Kremers WK, Alexander MP, et al. Using computer-assisted morphometrics of 5-year biopsies to identify biomarkers of late renal allograft loss. Am J Transplant. 2019. doi: 10.1111/ajt.15380.
28. Aboumsallem JP, Muthuramu I, Mishra M, Kempen H, De Geest B. Effective Treatment of Diabetic Cardiomyopathy and Heart Failure with Reconstituted HDL (Milano) in Mice. Int J Mol Sci. 2019;20(6). doi: 10.3390/ijms20061273.
29. Matthews DR, Hosker JP, Rudenski AS, Naylor BA, Treacher DF, Turner RC. Homeostasis model assessment: insulin resistance and beta-cell function from fasting plasma glucose and insulin concentrations in man. Diabetologia. 1985;28(7):412-9. doi: 10.1007/bf00280883.
30. Elsherbiny HE, Alexander MP, Kremers WK, Park WD, Poggio ED, Prieto M, et al. Nephron hypertrophy and glomerulosclerosis and their association with kidney

function and risk factors among living kidney donors. Clin J Am Soc Nephrol. 2014;9(11):1892-902. doi: 10.2215/CJN.02560314.
31. Weibel ER, Gomez DM. A principle for counting tissue structures on random sections. J Appl Physiol. 1962;17:343-8. doi: 10.1152/jappl.1962.17.2.343.
32. Fang JY, Lin CH, Huang TH, Chuang SY. In Vivo Rodent Models of Type 2 Diabetes and Their Usefulness for Evaluating Flavonoid Bioactivity. Nutrients. 2019;11(3). doi: 10.3390/nu11030530.
33. Surwit RS, Kuhn CM, Cochrane C, McCubbin JA, Feinglos MN. Diet-induced type II diabetes in C57BL/6J mice. Diabetes. 1988;37(9):1163-7. doi: 10.2337/diab.37.9.1163.
34. Breyer MD, Böttinger E, Brosius FC, Coffman TM, Harris RC, Heilig CW, et al. Mouse models of diabetic nephropathy. J Am Soc Nephrol. 2005;16(1):27-45. doi: 10.1681/ASN.2004080648.
35. Alpers CE, Hudkins KL. Mouse models of diabetic nephropathy. Curr Opin Nephrol Hypertens. 2011 May;20(3):278-84. doi: 10.1097/MNH.0b013e3283451901.
36. Haseyama T, Fujita T, Hirasawa F, Tsukada M, Wakui H, Komatsuda A, et al. Complications of IgA nephropathy in a non-insulin-dependent diabetes model, the Akita mouse. Tohoku J Exp Med. 2002;198(4):233-44. doi: 10.1620/tjem.198.233.
37. Balmer LA, Whiting R, Rudnicka C, Gallo LA, Jandeleit KA, Chow Y, et al. Genetic characterization of early renal changes in a novel mouse model of diabetic kidney disease. Kidney Int. 2019;96(4):918-26. doi: 10.1016/j.kint.2019.04.031.
38. Donegan D, Bale LK, Conover CA. PAPP-A in normal human mesangial cells: effect of inflammation and factors related to diabetic nephropathy. J Endocrinol. 2016;231(1):71-80. doi: 10.1530/JOE-16-0205.
39. Terami N, Ogawa D, Tachibana H, Hatanaka T, Wada J, Nakatsuka A, et al. Long-term treatment with the sodium glucose cotransporter 2 inhibitor, dapagliflozin, ameliorates glucose homeostasis and diabetic nephropathy in db/db mice. PLoS One. 2014;9(6):e100777. doi: 10.1371/journal.pone.0100777.
40. Vallon V, Gerasimova M, Rose MA, Masuda T, Satriano J, Mayoux E, et al. SGLT2 inhibitor empagliflozin reduces renal growth and albuminuria in proportion to hyperglycemia and prevents glomerular hyperfiltration in diabetic Akita mice. Am J Physiol Renal Physiol. 2014;306(2):F194-204. doi: 10.1152/ajprenal.00520.2013.
41. De Nicola L, Gabbai FB, Liberti ME, Sagliocca A, Conte G, Minutolo R. Sodium/glucose cotransporter 2 inhibitors and prevention of diabetic nephropathy: targeting the renal tubule in diabetes. Am J Kidney Dis. 2014;64(1):16-24. doi: 10.1053/j.ajkd.2014.02.010.
42. Hatanaka T, Ogawa D, Tachibana H, Eguchi J, Inoue T, Yamada H, et al. Inhibition of SGLT2 alleviates diabetic nephropathy by suppressing high glucose-induced oxidative stress in type 1 diabetic mice. Pharmacol Res Perspect. 2016;4(4):e00239. doi: 10.1002/prp2.239.
43. Malatiali S, Francis I, Barac-Nieto M. Insulin Prevents Hyperfiltration and Proteinuria but Not Glomerular Hypertrophy and Increases Mesangial Matrix Expansion in Diabetic Rats. Med Princ Pract. 2017;26(1):78-83. doi: 10.1159/000450864.
44. Ozluk Y, Blanco PL, Mengel M, Solez K, Halloran PF, Sis B. Superiority of virtual microscopy versus light microscopy in transplantation pathology. Clin Transplant. 2012;26(2):336-44. doi: 10.1111/j.1399-0012.2011.01506.x.
45. Jen KY, Olson JL, Brodsky S, Zhou XJ, Nadasdy T, Laszik ZG. Reliability of whole slide images as a diagnostic modality for renal allograft biopsies. Hum Pathol. 2013;44(5):888-94. doi: 10.1016/j.humpath.2012.08.015.
46. Bornfeldt KE, Kramer F, Batorsky A, Choi J, Hudkins KL, Tontonoz P, et al. A Novel Type 2 Diabetes Mouse Model of Combined Diabetic Kidney Disease and Atherosclerosis. Am J Pathol. 2018;188(2):343-52. doi: 10.1016/j.ajpath.2017.10.012.